

pubs.acs.org/JPCL Letter

Deep Learning Based Prediction of Perovskite Lattice Parameters from Hirshfeld Surface Fingerprints

Logan Williams, Arpan Mukherjee, and Krishna Rajan*



Cite This: J. Phys. Chem. Lett. 2020, 11, 7462-7468



Read Online

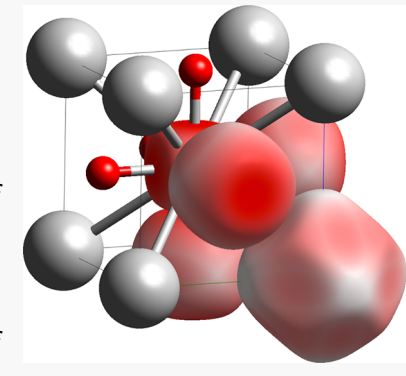
ACCESS

III Metrics & More



SI Supporting Information

ABSTRACT: This Letter describes the use of deep learning methods on Hirshfeld surface representations of crystal structure, as an automated means of predicting lattice parameters in cubic inorganic perovskites. While Hirshfeld Surface Analysis is a well-established tool in organic crystallography, we also introduce modified computational protocols for Hirshfeld Surface Analysis tailored specifically to account for nuanced but important differences dealing with inorganic crystals. We demonstrate how two-dimensional Hirshfeld surface fingerprints can serve as a rich "database" of information encoding the complexity of relationships between chemical bonding and bond geometry characteristics of perovskites. Our results are compared with other studies on lattice parameter prediction involving both experimental and computationally derived data, and it is shown that our approach is an improvement over other reported methods. The paper concludes by discussing how this work opens new avenues for data-driven high throughput computational predictions of structure—property relationships involving complex crystal chemistries.



The measurement and prediction of lattice parameters for perovskite structures has long been and continues to be a topic of study for many years. This arises from the fact that the lattice parameter serves as a probe into the complex geometric and bonding characteristics that govern the stability and properties of such compounds. The studies have mainly involved the statistical/machine learning-based analysis of experimental data, augmented by additional descriptor data such as atomic radii, Pauling electronegativities, and valence or oxidation states. 1-8 From a machine learning perspective, these studies utilized traditional algorithms such as Support Vector Regression (SVR), Artificial Neural Network (ANN), and General Regression Neural Network (GRNN). These have achieved high accuracy for experimentally realized cubic perovskites but are rarely tested against the wide chemical space that Density Functional Theory (DFT) can access. DFT is routinely used to predict many properties of materials, including lattice parameter, though the computationally cheapest and most popular functionals, the local-density approximation (LDA) and the generalized gradient approximation of Perdew-Burke-Ernzerhof (PBE) tend to underand overestimate the lattice constant, respectively.

More recently, methods such as the Crystal Graph Convolutional Neural Network (CGCNN) have been used to represent crystal structures for machine learning of various properties. The CGCNN method uses a graph network composed of atomic nodes containing elemental information and connections between nodes containing bond distances. A custom convolution function is used between connected nodes to incorporate environmental data on each node. The pool of neighbor-convoluted nodes is then summed and normalized to

create a 1D feature vector used to predict the property of interest for the crystal.

In this paper, we introduce an approach to predict lattice parameters in perovskite structures that is founded on a representation of crystal structure in terms of 3-dimensional (3D) Hirshfeld surfaces that encode both chemical bonding and molecular geometry information. 11 The concept of Hirshfeld surfaces is used extensively in the analysis of organic molecular crystals, 11-15 where it provides a computationally efficient way to analyze molecular packing, close contact points, molecule shape, and intermolecular interactions. Hirshfeld surfaces arise from the question of how to assemble molecules and fabricate flexible or rigid building blocks into multicomponent systems. In this study, we are expanding that concept to inorganic crystals, as it provides a viable framework as a representation that is sensitive to the crystal structure, stoichiometry (e.g., similar crystal structures may have different chemistries), defects, and lattice distortions associated with local site chemistry and occupancy.

For this study, we made some modifications to the traditional representations of the Hirshfeld surface used for molecular crystals. In smaller crystal systems, such as rocksalt, a traditional Hirshfeld surface will capture information about all

Received: July 19, 2020 Accepted: August 17, 2020



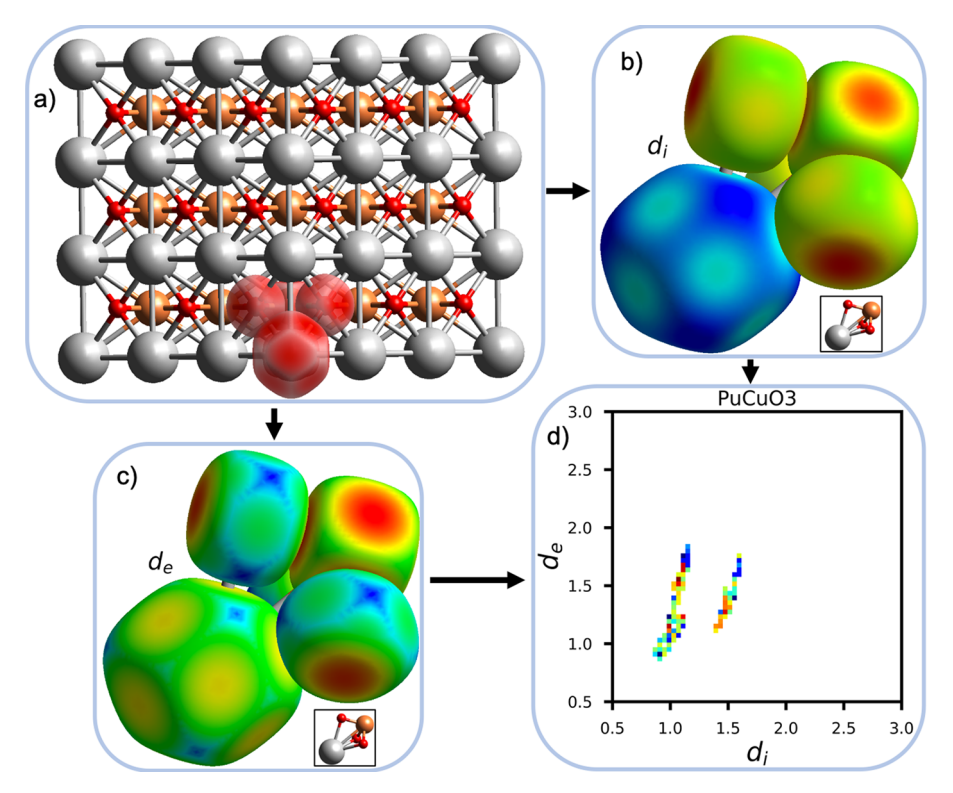


Figure 1. (a) Structure of $PuCuO_3$ using a lattice parameter of 3.52582 Å and the calculated Hirshfeld surfaces of the five atoms in the primitive unit cell shown in red. Lattice parameters used in calculation were randomly selected in the range 3.5–5.5 Å, the range most oxide cubic perovskites lie within. Gray atoms are Pu. Orange are Cu. Red are O. (b) Mapping of d_i onto the five Hirshfeld surfaces from (a) that compose the primitive unit cell of the structure. The inset shows the arrangement of the atoms under the surfaces. Dark blue to dark red spans 0.8425–1.5890 Å. (c) Mapping of d_e onto the five Hirshfeld surfaces from (a) that compose the primitive unit cell of the structure. The inset shows the arrangement of the atoms under the surfaces. Dark blue to dark red spans 0.8684–1.8699 Å. (d) Fingerprint plot of the combined five unique Hirshfeld surfaces of $PuCuO_3$, made by binning the (d_v, d_e) pairs, shown in (b) and (c), over all points on the surfaces. The fingerprint plot made by these atomic surfaces looks different from one made using one traditional Hirshfeld surface for the entire primitive cell. The differences and shared features are discussed more in the Supporting Information.

atoms. For larger systems, such as distorted or double perovskites, some atomic sites will be located deep inside a traditional Hirshfeld surface. Shifts of such deep sites contribute only very minimally to the shape of the Hirshfeld surface. Thus, those sites are poorly characterized within the fingerprint plot of the Hirshfeld surface. To address this issue, we chose to use a fingerprint made from the combined set of Hirshfeld surfaces for each unique atomic site within the crystal structure. This also removes the ambiguity of unit cell (or pro-molecule, in Hirshfeld surface terms) selection while allowing equal attention to all atoms within the crystal structure. Future work will elaborate upon the benefits this provides in larger and less symmetric crystal structures. The supplementary section compares traditional Hirshfeld surfaces and their fingerprint plots to this modified approach. The decision to use atomic Hirshfeld surfaces was inspired by the long history of Atom In Molecule (AIM) research utilizing Hirshfeld surfaces, 16-19 and our fingerprint acts as a Hirshfeld AIM characterization of the crystal system that is computationally simple through use of the neutral charge densities.

The Hirshfeld surface gives the shape of a molecule within an environment. It is calculated by taking, for all points in space, the sum of the spherically averaged electron densities for each atom within the molecule as well as each atom within a reasonable cutoff distance. The Hirshfeld surface is then defined as the points where 50% of the electron density comes from atoms within the molecule. Hirshfeld surfaces are thus a

function of the molecule's structure, atomic composition, and environment. In addition to the Hirshfeld surface itself, we can encode other geometric properties on the surfaces. In particular, each point on the surface can be mapped with a set of values based on the neighboring environment. The contact distances d_a and d_i are the distances from the Hirshfeld surface to the nearest atoms outside and inside the surface, respectively. The distribution of d_i and d_e in the fingerprint plot of a Hirshfeld surface characterizes the shape and environment of the molecule. It is desirable to have information on the shape and environment on each atom within the crystal structure when predicting the lattice parameter, or many other properties of inorganics. The lattice parameter of a crystal is a complex function of the chemistry and crystal structure. Directional bonding and orbital hybridization can cause the same atom to behave very differently in different local environments. Atomic properties and bonding interactions between neighbor atoms make every atom and every atom's environment critical to the determination of the lattice parameter. For this reason, as noted above, we have chosen to use an alternate fingerprint plot consisting of the summed (d_i, d_e) pairs from all atomic Hirshfeld surfaces within the crystal structure, as shown in Figure 1.

In this study, we show how Hirshfeld surfaces provide a simple but powerful method of "fingerprinting" an inorganic crystal for machine learning techniques. The 3D Hirshfeld surface can be converted into a rotationally invariant two-

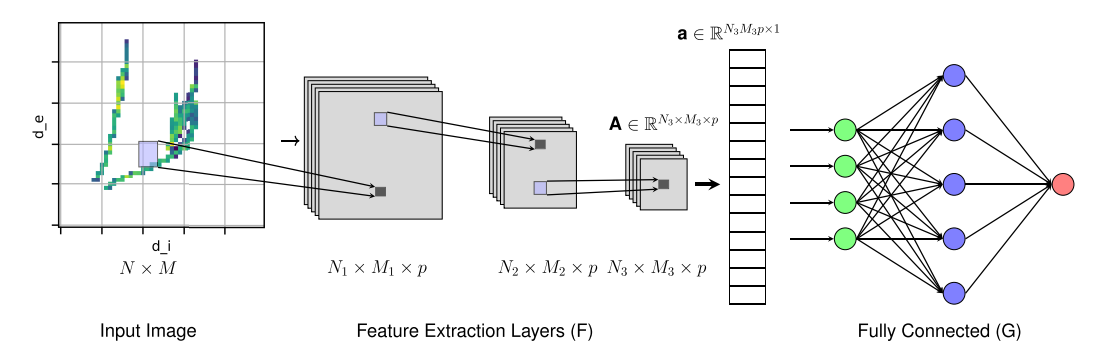


Figure 2. Feed-forward propagation of our proposed neural network has feature extraction layers (F) and fully connected layers (G) that uses a 2D fingerprint plot of size $N \times M$ as an input. The feature extraction layers (F) use a combination of convolution, ReLU, and pooling layers to produce low-dimensional feature maps that shows distinct regions in the image. The final p set of feature maps $\mathbf{A} = \{A_1, A_2, \ldots, A_p\}$, $A_k \in \mathbb{R}^{N_3 \times M_3}$, when flattened produces a 1D feature vector $\mathbf{a} \in \mathcal{R}^{N_3 M_3 p}$ that serves as input for the fully connected layers (G). The output of the network $y \in \mathbb{R}$ (in red) is a scalar quantity that represents the lattice parameter.

dimensional (2D) "fingerprint" by measuring $(d_{i\nu} d_{e})$ at each point on the surface and binning these pairs into a 2D histogram. These fingerprints have the same format as single-channel 2D images (a 2D tensor representing a regular grid of magnitude values, such as a grayscale image or a height map) and are well suited as input to neural network image processing techniques such as Convolutional Neural Networks.

In this paper, we use our fingerprint plot made from atomic Hirshfeld surfaces to predict the DFT lattice constants for ABO₃ cubic perovskites, to demonstrate the capability of the method for general machine learning of crystal properties. For comparison, we have also used the Crystal Graph Convolutional Neural Network (CGCNN) technique. We use the set of ABO₃ cubic perovskite structures and their relaxed lattice constants from the Open Quantum Materials Database OQMD²² to demonstrate that a neural net trained on the atomic Hirshfeld surface fingerprint plots achieves an accuracy on par or better than the CGCNN technique.

To generate our data set, the 5321 ABO₃ cubic perovskites from OQMD were initially selected. These include all elements up to Z = 94 except for the noble gases, the halogens, H, C, N, O, P, S, Se, and Po. The data set was then trimmed down to 5250 structures by removing cases fitting either of two criteria. First, if the relaxed lattice parameter was greater than 5 Å or more than 2% larger than the (generous) unrelaxed lattice parameter used by OQMD, they were removed as these are likely to be unstable structures. Second, if the relaxed lattice parameter was equal to the unrelaxed lattice parameter, they were removed as these may be unnoticed failed calculations. The Hirshfeld surface of each atom in every structure was then calculated using the Tonto software package, an open-source tool for Hirshfeld surface and other analysis.²³ For both Hirshfeld surface calculation and CGCNN initialization, initial lattice constants were assigned to each structure as a random value in the range of 3.5-5.5 Å, the range of most oxide cubic perovskites. A second data set using the OQMD unrelaxed lattice parameters (based on stoichiometry) is also included in the Supporting Information, as well a demonstration of the technique's robustness against variation in initial lattice parameter. To achieve smooth fingerprint plots, the atomic Hirshfeld surfaces were interpolated using 10 points between each vertex, and then the fingerprint plot for each structure was created by binning the (d_i, d_e) pairs of all interpolated surfaces in the structure into 50×50 bin histograms (bin size = 0.04) Å) ranging 0.76–2.8 Å for both d_i and d_e . Additional example

structures and Hirshfeld surfaces are shown in the Supporting Information.

The machine learning model used in this work is a CNN-based regression model that takes a conventional $ConvNet^{24}$ and replaces the last softmax layer with a dense layer of a single output variable. The feature-extraction layers (F) contains Convolution + ReLU. See Figure 2. The exact architecture is listed in the Supporting Information.

Convolution Neural Networks (CNN) work on an input variable that is a tensor having a grid-like structure. The underlying assumption is that the complex geometrical features of a tensor are an ensemble of smaller and simpler patterns. In contrast to any other type of layer, CNN uses small filters that extract local features and progressively reduce the size of the input variable with each layer. The number of layers in CNN increases with an increase in the size of the input tensor. However, the number of parameters increases linearly with an increase in the number of layers, since the previous layer can have the same number of parameters as the next layer. Thus, CNN exhibits both low space and computational time complexity for larger input sizes.

Consider the input image X of size $N\times M$ and the parameter set of R as θ . Each convolution + ReLU and pooling layer produces feature maps of reduced dimension as compared to its input. The output feature map of a layer serves as the input for the next layer. Consider the input to the ith layer as $A_i\in\mathbb{R}^{N_i\times M_i}$ as input to the convolution layer F_i with $w_i\in\mathbb{R}^{p_i^i\times p_2^i}$ as one of the filter. The pixel value of feature map $A_{i+1}\in\mathbb{R}^{N_i-p_1^i+1\times M_i-p_2^i+1}$ at m, n produced by the convolution layer is given as

$$A_{i+1}[m, n] = (A_i \times F_i)[m, n]$$

$$= \sum_{j} \sum_{k} w_i[j, k] A_i[m - j, n - k]$$

 A_{i+1} goes through the Rectified Linear Unit (ReLU) function as $A_{i+1} = \max(0, A_{i+1})$. Thus, the convolution layer works by identifying features of size $p_1^i \times p_2^i$ as produced by the filter w_i is activated only where there is a positive output. Finally, a maxpooling layer of size $q_1^i \times q_1^i$ reduces the dimension of the feature map A_{i+1} to size $N_{i+1} \times M_{i+1}$, where

Table 1. \hat{r}^2 Value, Mean Absolute Error (MAE), and Mean Squared Error (MSE) for Test Set Prediction Using Existing Literature Approaches Compared to Our Atomic Hirshfeld Surfaces Fingerprint Plot with a Convolutional Neural Network, Which Shows Higher Accuracy

data set	data type	method	\hat{r}^2	MAE	MSE
OQMD - random a ^a	computational	CGCNN ¹⁰	0.948341	0.0402052	0.00401756
Kuzmanovski et al. ⁵	experimental	counter-propagation artificial neural network (CPANN) ⁵	0.931182	0.0853067	0.01230575
OQMD - random a ^a	computational	fingerprint + CNN	0.974527	0.0333193	0.00198105
Kuzmanovski et al. ⁵	experimental	fingerprint + CNN	0.993874	0.0220539	0.00109539

"The "OQMD - random a" data set refers to the data set constructed from cubic oxide perovskites calculated in OQMD, 22 with their initial lattice parameters randomized in the 3.5-5.5 Å range, as described in the main text.

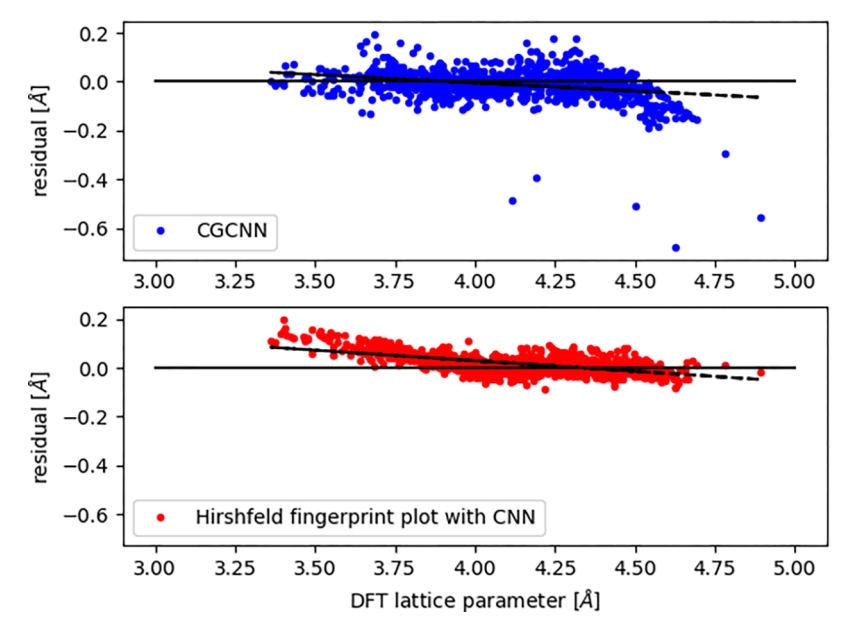


Figure 3. Test set residuals for the prediction of cubic perovskite DFT lattice parameters from structures with randomized lattice parameters using (top) the CGCNN technique ¹⁰ or (bottom) the atomic Hirshfeld surfaces fingerprint plot with a convolutional neural network. The fingerprint plot method shows better performance with no large outliers. The dashed lines show a linear regression of the residuals.

$$N_{i+1} = \frac{N_i - p_1^i + 1}{q_1^i}$$
 $M_{i+1} = \frac{M_i - p_2^i + 1}{q_2^i}$

Apart from the dimensionality reduction, the max-pooling also produces an output map that is invariant to small transformation within the pool window. The output neuron $y \in \mathbb{R}$ of the model is a scalar quantity representing the lattice parameter. Considering the estimated output of the model as \hat{y} and the target value as y, the regression loss function can be written as

$$L = \frac{1}{N} \sum_{i}^{N} (y_{i} - \hat{y}_{i})^{2} = \frac{1}{N} \sum_{i}^{N} (y_{i} - R_{\theta}(X))^{2}$$

The model parameters are trained via back-propagation using the Adam optimizer^{2,5} as

$$\hat{\theta} = \min_{\theta} L = \min_{\theta} \frac{1}{N} \sum_{i}^{N} (y_{i} - R_{\theta}(X))^{2}$$

The model is trained on an environment with Intel i7-7920HQ CPU, 32 GB RAM with a Nvidia Quadro M2200 video card using the open source library Keras with Tensorflow v1.8.0 backend.²⁶

Our convolutional neural net and the CGCNN were trained and tested using the same train/test split. As shown in Table 1 and Figure 3, the Hirshfeld surfaces fingerprint plus CNN achieves higher accuracy than the CGCNN method, indicating that Hirshfeld surface shape changes are sufficiently information-rich to provide accurate property predictions across wide chemical spaces.

Clearly, the high level of statistical fit reflects the richness of information that is embedded in the 2-dimensional Hirshfeld surface fingerprints. As noted earlier, it encodes both chemical bonding and molecular geometry information. This genre of data representation simultaneously captures the synergistic effects of chemical formulas, bonding, electronic structure, intermolecular packing, the nature of the structural building units, and their network connections, all of which influence lattice parameter. The CNN is specifically selecting features in the 2D HS which are in fact the 2D statistical distributions in d_i vs d_e . So our analysis is suggesting that certain (d_v, d_e) distributions hold the key to predicting the lattice parameter. (d_i, d_e) distributions represent information on bond contacts, and hence it is not unreasonable that it serves as a good surrogate indicator of lattice parameters. In a follow up publication, we shall provide a more detailed documentation of the correlations and trends between (d_i, d_e) distributions associated with the different lattice parameter variations.

To test the method against experimental data, small data sets, and non-oxides as well, the data set of Kuzmanovski et al.⁵ was also used. To create easier training for the small data set,

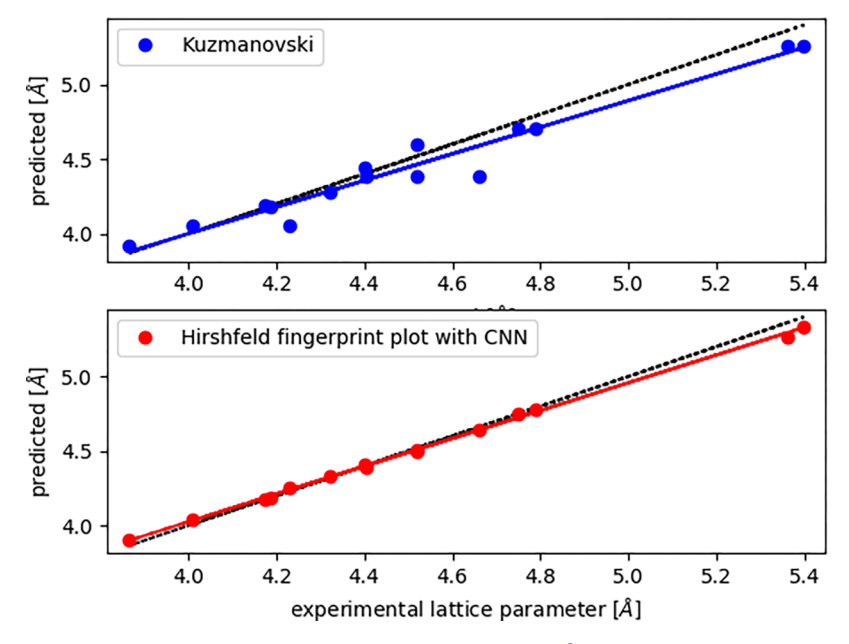


Figure 4. Predicted vs actual plots for the test set of the data set from Kuzmanovski et al. using (top) their predictions and (bottom) the Hirshfeld surfaces fingerprint plus Convolutional Neural Network approach. \hat{r}^2 of the prediction to true values is 0.9939 for the HFS+CNN and 0.9312 for Kuzmanovski's method. The r value of 0.976 ($\hat{r}^2 = 0.952$) in their paper referred to the fit of the regression to the prediction values, not the prediction values to the true values.

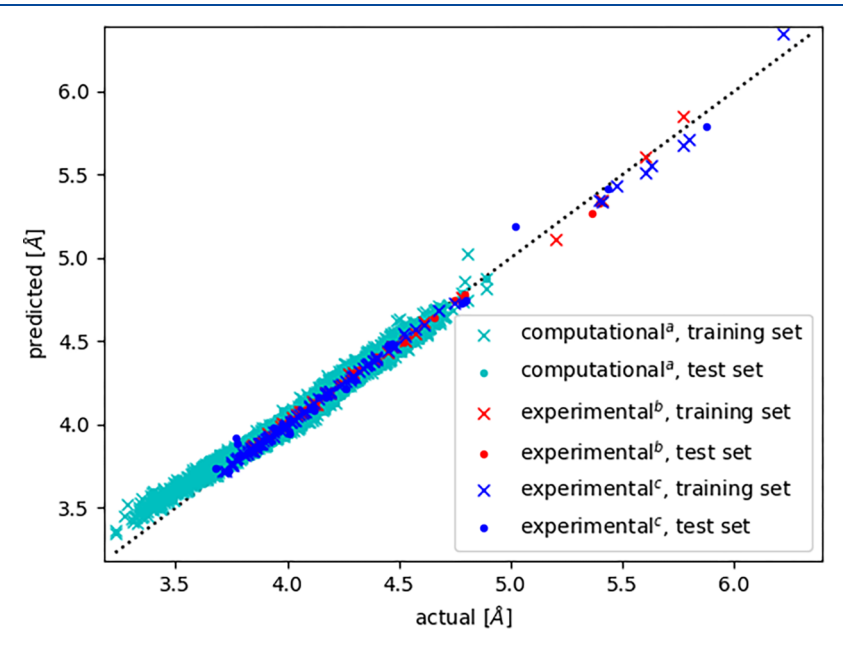


Figure 5. Plot collecting the results of the Hirshfeld surfaces fingerprint plot + CNN on (a) the OQMD (with randomized lattice parameter input), (b) Kuzmanovski, and (c) Sidey (discussed in the Supporting Information) data sets.

the initial lattice parameter for all structures was set to 4.5 Å during Hirshfeld surface generation. As shown in Table 1 and Figure 4, the Hirshfeld surfaces fingerprint method produces far more accurate predictions than Kuzmanovski's method built on ionic radii, oxidation state, and electronegativity, again reinforcing our earlier comments on the richness of information embedded in Hirschfeld surface representation of crystal structures. The prediction vs observed values for the previously discussed data sets, including test and training sets, as well as another discussed in the Supporting Information, are shown in Figure 5, demonstrating excellent performance on multiple data sets.

In this paper we have demonstrated that Hirshfeld surface fingerprints provide a powerful representation of perovskite crystal chemistry that is well suited for the application of deep learning methods to predict lattice parameters. Since Hirshfeld surfaces contain not only all of the geometric information of a compound but also chemistry and bonding information, they can serve as a rich information landscape on which machine learning tools can be applied.²⁷ The results described in this paper lay the foundation for exploiting this genre of data motif to predict other properties and can be readily generalized to exploring an entire genre of complex inorganic solids, which will be described in forthcoming publications.

ASSOCIATED CONTENT

Supporting Information

The Supporting Information is available free of charge at https://pubs.acs.org/doi/10.1021/acs.jpclett.0c02201.

OQMD data (TXT)

Brief overview of Hirshfeld surfaces, comments on the modified fingerprint plot based on atomic Hirshfeld surfaces and comparisons to the traditional fingerprint plot, example fingerprint plots of various studied perovskites, a discussion on patterns in the fingerprint plots and the effect of the lattice parameter used in their generation, detailed neural network architecture, results for additional data sets, and breakdown of OQMD data set results by periodic table group and row number for both the A and the B site (PDF)

AUTHOR INFORMATION

Corresponding Author

Krishna Rajan — Department of Materials Design and Innovation, University at Buffalo, Buffalo, New York 14260-1660, United States; orcid.org/0000-0001-9303-2797; Email: krajan3@buffalo.edu

Authors

Logan Williams — Department of Materials Design and Innovation, University at Buffalo, Buffalo, New York 14260-1660, United States; orcid.org/0000-0002-9062-8293

Arpan Mukherjee — Department of Materials Design and Innovation, University at Buffalo, Buffalo, New York 14260-1660, United States; orcid.org/0000-0001-5698-6268

Complete contact information is available at: https://pubs.acs.org/10.1021/acs.jpclett.0c02201

Notes

The authors declare no competing financial interest.

ACKNOWLEDGMENTS

The authors acknowledge the support from NSF Award# 1640867 - DIBBs: EI: Data Laboratory for Materials Engineering and the Collaboratory for a Regenerative Economy (CoRE center) in the Dept. of Materials Design and Innovation - University at Buffalo.

REFERENCES

- (1) Javed, S. G.; Khan, A.; Majid, A.; Mirza, A. M.; Bashir, J. Lattice Constant Prediction of Orthorhombic ABO3 Perovskites Using Support Vector Machines. *Comput. Mater. Sci.* **2007**, 39 (3), 627–634.
- (2) Majid, A.; Khan, A.; Javed, G.; Mirza, A. M. Lattice Constant Prediction of Cubic and Monoclinic Perovskites Using Neural Networks and Support Vector Regression. *Comput. Mater. Sci.* **2010**, *50* (2), 363–372.
- (3) Jiang, L. Q.; Guo, J. K.; Liu, H. B.; Zhu, M.; Zhou, X.; Wu, P.; Li, C. H. Prediction of Lattice Constant in Cubic Perovskites. *J. Phys. Chem. Solids* **2006**, *67* (7), 1531–1536.
- (4) Moreira, R. L.; Dias, A. Comment on "Prediction of Lattice Constant in Cubic Perovskites. *J. Phys. Chem. Solids* **2007**, *68* (8), 1617–1622.
- (5) Kuzmanovski, I.; Dimitrovska-Lazova, S.; Aleksovska, S. Examination of the Influence of Different Variables on Prediction of Unit Cell Parameters in Perovskites Using Counter-Propagation Artificial Neural Networks. *J. Chemom.* **2012**, *26* (1–2), 1–6.

- (6) Ubic, R. Revised Method for the Prediction of Lattice Constants in Cubic and Pseudocubic Perovskites. *J. Am. Ceram. Soc.* **2007**, *90* (10), 3326–3330.
- (7) Verma, A. S.; Jindal, V. K. Lattice Constant of Cubic Perovskites. *J. Alloys Compd.* **2009**, 485 (1–2), 514–518.
- (8) Sidey, V. A Simplified Empirical Model for Predicting the Lattice Parameters of the Cubic/Pseudocubic Perovskites. *J. Solid State Chem.* **2019**, *279* (September), 120951.
- (9) Zhang, G.-X.; Reilly, A. M.; Tkatchenko, A.; Scheffler, M. Performance of Various Density-Functional Approximations for Cohesive Properties of 64 Bulk Solids. *New J. Phys.* **2018**, 20 (6), 063020.
- (10) Xie, T.; Grossman, J. C. Crystal Graph Convolutional Neural Networks for an Accurate and Interpretable Prediction of Material Properties. *Phys. Rev. Lett.* **2018**, *120* (14), 145301.
- (11) Spackman, M. A.; Jayatilaka, D. Hirshfeld Surface Analysis. CrystEngComm 2009, 11 (1), 19–32.
- (12) Jotani, M. M.; Lee, S. M.; Lo, K. M.; Tiekink, E. R. T. 1-Chloro-4-[2-(4-Chlorophenyl)Ethyl]Benzene and Its Bromo Analogue: Crystal Structure, Hirshfeld Surface Analysis and Computational Chemistry. *Acta Crystallogr. Sect. E Crystallogr. Commun.* **2019**, 75 (5), 624–631.
- (13) Jelsch, C.; Bibila Mayaya Bisseyou, Y. Atom Interaction Propensities of Oxygenated Chemical Functions in Crystal Packings. *IUCrJ* **2017**, 4 (2), 158–174.
- (14) Spackman, P. R.; Thomas, S. P.; Jayatilaka, D. High Throughput Profiling of Molecular Shapes in Crystals. *Sci. Rep.* **2016**, *6* (1), 22204.
- (15) Tan, S. L.; Jotani, M. M.; Tiekink, E. R. T. Utilizing Hirshfeld Surface Calculations, Non-Covalent Interaction (NCI) Plots and the Calculation of Interaction Energies in the Analysis of Molecular Packing. *Acta Crystallogr. Sect. E Crystallogr. Commun.* **2019**, 75 (3), 308–318.
- (16) Bultinck, P.; Van Alsenoy, C.; Ayers, P. W.; Carbó-Dorca, R. Critical Analysis and Extension of the Hirshfeld Atoms in Molecules. *J. Chem. Phys.* **2007**, *126* (14), 144111.
- (17) Tkatchenko, A.; Scheffler, M. Accurate Molecular Van Der Waals Interactions from Ground-State Electron Density and Free-Atom Reference Data. *Phys. Rev. Lett.* **2009**, *102* (7), 073005.
- (18) Ambrosetti, A.; Reilly, A. M.; DiStasio, R. A.; Tkatchenko, A. Long-Range Correlation Energy Calculated from Coupled Atomic Response Functions. *J. Chem. Phys.* **2014**, *140* (18), 18A508.
- (19) Bučko, T.; Lebègue, S.; Angyán, J. G.; Hafner, J. Extending the Applicability of the Tkatchenko-Scheffler Dispersion Correction via Iterative Hirshfeld Partitioning. *J. Chem. Phys.* **2014**, *141* (3), 034114.
- (20) Frid-Adar, M.; Diamant, I.; Klang, E.; Amitai, M.; Goldberger, J.; Greenspan, H. GAN-Based Synthetic Medical Image Augmentation for Increased CNN Performance in Liver Lesion Classification. *Neurocomputing* **2018**, *321*, *321*–*331*.
- (21) Ge, L.; Liang, H.; Yuan, J.; Thalmann, D. Robust 3D Hand Pose Estimation From Single Depth Images Using Multi-View CNNs. *IEEE Trans. Image Process.* **2018**, 27 (9), 4422–4436.
- (22) Saal, J. E.; Kirklin, S.; Aykol, M.; Meredig, B.; Wolverton, C. Materials Design and Discovery with High-Throughput Density Functional Theory: The Open Quantum Materials Database (OQMD). *JOM* **2013**, *65* (11), 1501–1509.
- (23) Jayatilaka, D.; Grimwood, D. J. Tonto: A Fortran Based Object-Oriented System for Quantum Chemistry and Crystallography. In *Computational Science ICCS 2003*; Sloot, P. M. A., Abramson, D., Bogdanov, A. V, Gorbachev, Y. E., Dongarra, J. J., Zomaya, A. Y., Eds.; Springer: Berlin, Heidelberg, 2003; pp 142–151.
- (24) Simonyan, K.; Zisserman, A. Very Deep Convolutional Networks for Large-Scale Image Recognition. *arXiv Prepr.* arXiv1409.1556 **2014**.
- (25) Kingma, D. P.; Ba, J. Adam: A Method for Stochastic Optimization. arXiv Prepr. arXiv1412.6980 2014.
- (26) Abadi, M.; Agarwal, A.; Barham, P.; Brevdo, E.; Chen, Z.; Citro, C.; Corrado, G. S.; Davis, A.; Dean, J.; Devin, M. Tensorflow: Large-

Scale Machine Learning on Heterogeneous Distributed Systems. arXiv Prepr. arXiv1603.04467 **2016**.

(27) Shen, X.; Zhang, T.; Broderick, S.; Rajan, K. Correlative Analysis of Metal Organic Framework Structures through Manifold Learning of Hirshfeld Surfaces. *Mol. Syst. Des. Eng.* **2018**, 3 (5), 826–838.